Vol. 736: 47–62, 2024
https://doi.org/10.3354/meps14588

MARINE ECOLOGY PROGRESS SERIES
Mar Ecol Prog Ser

Published May 23

Eelgrass meadow response to heat stress. II. Impacts of ocean warming and marine heatwaves measured by novel metrics

Amelie C. Berger[1,*], Peter Berg[1], Karen J. McGlathery[1], Lillian R. Aoki[2], Kylor Kerns[1]

[1]Department of Environmental Sciences, University of Virginia, Charlottesville, VA 22903, USA
[2]Department of Environmental Studies, University of Oregon, Eugene, OR 97403, USA

ABSTRACT: In June 2015, a marine heatwave triggered a severe eelgrass *Zostera marina* die-off event at the Virginia Coast Reserve (USA), followed by a slow and spatially heterogeneous recovery. We investigated the effects of heat stress on seagrass loss and recovery. Using hourly summer water temperature measurements from 2016–2020, we developed a novel approach to quantifying the stress of ocean warming on seagrass meadows. We defined 2 metrics: cumulative heat stress (as heating degree-hours, HDHs) and heat stress relief (as cooling degree-hours, CDHs), relative to a 28.6°C eelgrass ecosystem thermal tolerance threshold previously determined at this site from aquatic eddy covariance measurements. These metrics were compared to spatiotemporal patterns of summertime eelgrass shoot density and length. We found that the healthiest parts of the meadow benefited from greater heat stress relief (2–3×) due to tidal cooling (inputs of cooler ocean water through ocean inlets) during warm periods, resulting in ~65% higher shoot densities compared to the center of the meadow, which experienced higher heat stress (2×) and less relief. We also calculated the amount of heat stress preceding the eelgrass die-off in summer 2015, and found that this event was triggered by a cumulative heat stress of ~100–200°C-hours during the peak growing season. Sulfur isotope analyses of eelgrass leaves and sediment also suggested that sulfide toxicity likely contributed to eelgrass decline. Overall, our metrics incorporate physiological heat tolerances with the duration and intensity of heat stress and relief, and thus lay the groundwork for forecasting seagrass meadow vulnerability and resilience to future warming oceans.

KEY WORDS: Heat stress · Resilience · Sulfide toxicity · Eelgrass · *Zostera marina* · Marine heatwaves · Ocean warming · Metrics · Seagrass recovery

1. INTRODUCTION

Climate change is a major threat to coastal ecosystems worldwide. In the past few decades, the increased occurrence of extreme heating events, such as marine heatwaves — periods of at least 5 consecutive days when water temperatures exceed a local climatological threshold (90th percentile of 30 yr temperature data, Hobday et al. 2016) — has led to dramatic changes in the biodiversity, distributional range, and physiological function of marine foundation species and habitats (e.g. Wernberg et al. 2016, Smale et al. 2019). These events can have devastating impacts on marine ecosystems, such as mass coral bleaching (e.g. Skirving et al. 2019, Duarte et al. 2020) and widespread declines in kelp forests (e.g. Wernberg et al. 2016, Thomsen et al. 2019) and seagrass meadows (e.g. Thomson et al. 2015, Arias-Ortiz et al. 2018, Berger et al. 2020). Such declines are of significant concern globally as coastal ecosystems support commercially important fisheries and local economies (e.g. Costanza et al. 1997, Nagelkerken et al. 2000, Rees et al. 2010), protect coastlines (Koch et al. 2009), and play an important role in biogeochemical cycling and maintaining water quality (e.g. Mateo et al. 2003, Armitage & Fourqurean 2016, Aoki et al. 2020a). Sea-

*Corresponding author: acb4rk@virginia.edu

Publisher: Inter-Research · www.int-res.com

grass meadows in particular are important 'blue' carbon sinks in the global carbon cycle (Fourqurean et al. 2012, Oreska et al. 2017, Macreadie et al. 2019). However, extreme warming events can lead to widespread seagrass loss, and may trigger a rapid and substantial release of CO_2 due to remineralization of buried organic matter (Pendleton et al. 2012, Arias-Ortiz et al. 2018, Smale et al. 2019, Aoki et al. 2021). As continued ocean warming and increased frequency of marine heatwaves are predicted through the 21st century (Frölicher et al. 2018, Oliver et al. 2019), it is critical to better understand heat stress impacts on seagrass meadows.

Seagrass die-off events can occur when water temperatures exceed the thermal tolerance limits of the species (e.g. Moore & Jarvis 2008, Marbá & Duarte 2010, Arias-Ortiz et al. 2018, Berger et al. 2020). Beyond a certain optimum temperature threshold (T_{th}), increasing temperatures damage the photosynthetic apparatus of the plants (Wahid et al. 2007, York et al. 2013). This leads to a decrease in photosynthesis and, because respiration is concurrently stimulated, ultimately a carbon deficit in the plant that causes reduced growth and biomass loss (Moore & Short 2006, Lee et al. 2007, Collier et al. 2011, Ewers 2013). The temperature threshold for an eelgrass *Zostera marina* meadow at the Virginia Coast Reserve (VCR), USA, was recently determined to be 28.6°C, based on *in situ* aquatic eddy covariance measurements of eelgrass ecosystem metabolism and temperature under naturally varying environmental conditions (Berger & Berg 2024, this volume). The VCR is located at the southern edge of the eelgrass range on the US Atlantic coast (Moore & Short 2006), an area that has already experienced high temperature-related die-off events (Moore & Jarvis 2008, Shields et al. 2019, Berger et al. 2020) and is therefore particularly vulnerable to future warming. The most recent die-off event occurred as a result of a marine heatwave at the VCR in June 2015 (Berger et al. 2020, Aoki et al. 2021). The substantial loss of eelgrass biomass that summer was followed by several years of spatially heterogeneous recovery within the meadows, suggesting complex and spatially varying heat stress dynamics.

While it has been established that the eelgrass die-off resulted from an increased frequency of temperatures above T_{th} in June 2015 compared to other years (Berger et al. 2020), little is known about how the duration and intensity of heat stress affect eelgrass loss and recovery, and how these factors might vary spatially within a meadow. In the coral literature, the intensity and duration of heat stress are described using 'degree heating weeks' as a metric to predict coral bleaching and mortality (Liu et al. 2014, Hughes et al. 2017). This metric is a measure of the heating above a local threshold — maximum monthly sea surface temperature (SST) based on long-term records — where the temperature anomalies above this threshold are cumulated. A similar metric is needed for seagrass ecosystems to predict the impact of ocean warming and extreme heating events.

Seagrass mortality as a result of high water temperatures may be exacerbated by other stressors such as episodic turbidity and sulfide intrusion, both of which have direct negative impacts on seagrass survival (e.g. Greve et al. 2003, Borum et al. 2005, Moore & Jarvis 2008, Moore et al. 2014). Sulfide is produced by sulfate-reducing bacteria in anoxic sediments and, if it diffuses into seagrass tissues, can suppress photosynthesis and growth, ultimately leading to seagrass mortality (e.g. Pedersen et al. 2004, Borum et al. 2005, Calleja et al. 2007). This may occur during periods of hypoxia or warming when the oxygen demand from the plants, the sediments, and the water column is high (e.g. Holmer & Nielsen 1997, Greve et al. 2003, Frederiksen & Glud 2006). This sulfide intrusion is reflected in the sulfur isotopic signatures ($\delta^{34}S$) of seagrass tissues (e.g. Frederiksen et al. 2006).

Our goal in this study was 2-fold. To better understand the response of eelgrass meadows to heat stress, we formulated 2 heat stress metrics that account for the intensity and duration of heating and cooling relative to the local eelgrass ecosystem temperature stress threshold (28.6°C, Berger & Berg 2024). These metrics were applied to 4 yr of continuous summer water temperature data to understand how temperature stress and relief affected eelgrass loss and recovery patterns at our study site following the die-off event in 2015 (Berger et al. 2020, Aoki et al. 2021). We further investigated potential synergistic effects between heat stress and sulfide intrusion on eelgrass resilience.

2. MATERIALS AND METHODS

2.1. Study site

The VCR Long-Term Ecological Research (VCR-LTER) site hosts one of the largest successful eelgrass restoration projects globally (Orth & McGlathery 2012, Orth et al. 2020). Since 2001, over 70 million seeds have been broadcast in 4 shallow subtidal coastal bays on the Atlantic side of the Delmarva peninsula (Orth et al. 2006, 2020). South Bay contains the largest of these restored eelgrass meadows (~20 km^2

as of 2018, Orth et al. 2020). This meadow is situated between a barrier island to the east and a channel to the west, and is connected to the Atlantic Ocean by 2 inlets north and south of the meadow (Fig. 1). The eelgrass growing in South Bay is doing so under favorable water quality, light, and hydrodynamic conditions (Lawson et al. 2007, Moore et al. 2012, Oreska et al. 2021), in large part due to the limited human population and development in this region, combined with the lack of freshwater runoff into the coastal bays and the sheltering of the lagoons by barrier islands. This study system is therefore ideal for studying the isolated effects of warming on eelgrass meadows. Mean water depth in South Bay is 1.2 m with a tidal range of 1 m (semi-diurnal tides, Fagherazzi & Wiberg 2009). Sediments in South Bay are predominantly sandy with a mean grain size of 71 µm (Lawson et al. 2012, Oreska et al. 2017).

In June 2015, the coastal bays at the VCR experienced a marine heatwave, which led to a ~90% decline in eelgrass biomass in regions of South Bay (Berger et al. 2020, Aoki et al. 2021). Long-term eelgrass monitoring efforts captured this die-off and the partial recovery in restoration plots in the center of the meadow. Aerial imagery and expanded eelgrass monitoring after the die-off revealed heterogeneous patterns in eelgrass cover, with lower shoot densities in the center compared to the outer portions of the meadow (see below). This implied there was a difference in exposure to heat stress within the meadow, and prompted our efforts to better understand the relationship between temperature and eelgrass loss and recovery at the landscape scale.

To do this, we conducted a pilot study in June and July 2016 (1 yr after the 2015 die-off event) where we set up a network of 4 temperature-monitoring sites along a north–south transect in South Bay, spanning the length of the meadow from the center (site 0, Fig. 1) towards the northern and southern inlets. The following year (2017), we increased the spatial resolution of this network by adding 5 more sites, for a total of 9 sites where we monitored summer (May–August) water temperatures until 2020 (Fig. 1).

Eelgrass shoot density counts and length measurements were made at 5 of the 9 sites during summer 2019. Sites in the southern portion of South Bay (negative numbers, Fig. 1) were included in our temperature analyses but were excluded from our eelgrass measurements due to differences in depth and turbidity to avoid confounding factors when relating the eelgrass metrics to temperature stress. These sites were at or below a 1.5 m mean depth limit determined for eelgrass in the coastal bays at the VCR (Aoki et al. 2020b). The northernmost site (site 5, Fig. 1) represents the northern edge of the meadow and was also too deep to sustain dense eelgrass. It was therefore excluded from our eelgrass density and length measurements. Sites 0 and 4 (Fig. 1) have been part of other studies (Berger et al. 2020, Berger & Berg 2024) and are considered the end members of a temperature gradient identified during our 2016 pilot study. Site 0 ('center site', 37° 15′ 43.6″ N, 75° 48′ 54.6″ W), is located in the less dense, patchier center of the meadow in which severe marine heatwave effects were observed (Aoki et al. 2021), and site 4 ('northern site', 37° 16′ 34.2″ N, 75° 48′ 44.4″ W) is located in the northern, denser part of the meadow where we hypothesize the proximity to the ocean inlet mediated the effects of the marine heatwave through tidal cooling (Fig. 1). We therefore focused on these 2 sites

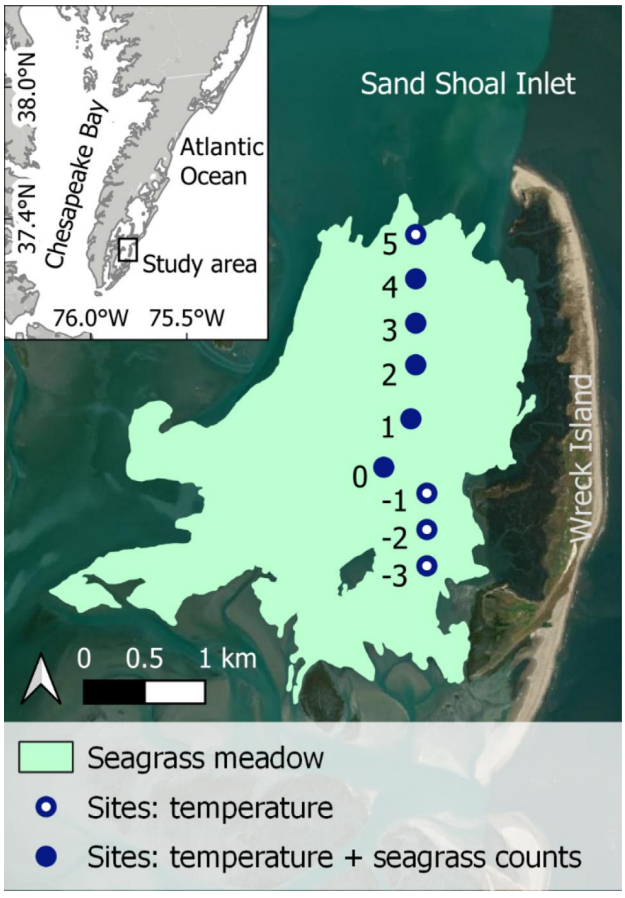

Fig. 1. Study sites in the South Bay eelgrass meadow at the Virginia Coast Reserve Long-Term Ecological Research (VCR-LTER) site. Summer water temperatures were measured from 2017 to 2020 at all 9 sites. Eelgrass shoot densities were counted every ~2 wk during summer 2019 at 5 of the 9 sites, along the center–north transect (filled-in circles). Numbers represent site position along the north–south transect in the meadow

for most of our comparisons of heat stress and eelgrass metrics. Berger & Berg (2024) showed similar water depth and light availability between the center and northern part of the meadow.

2.2. Water and sediment temperature measurements

HOBO Pendant® temperature loggers (accuracy ±0.53°C and precision = 0.14°C, Onset®) recorded water temperature every 10 min at each site within the eelgrass canopy (20 cm above the sediment surface). The 10 min data were then averaged to produce an hourly water temperature record. Table 1 lists measurement dates and the resulting number of hours in our record for each year, including our shorter pilot study in 2016.

In August 2018, we also investigated temperature stratification in the sediment and water column by placing temperature loggers 2.5 and 5 cm below the sediment surface and 2.5, 5, 10, 20, 30, 60, and 120 cm above the sediment surface at sites 0 and 4 for 20 d. We performed 1-way ANOVAs on the temperature records from each site to determine whether temperature varied between the water column (30 cm above the sediment surface) and the 2 sediment depths (−2.5 and −5 cm) (n = 2874 hourly observations). We also examined how much attenuation occurred in maximum daily temperatures between the water column and the sediment through 1-way repeated measures ANOVAs on the daily temperature maxima at each site. We used post hoc pairwise *t*-tests with adjusted p-values to evaluate mean temperature differences between depths when significant effects ($p < 0.05$) were found in the ANOVAs.

Prior to each deployment, HOBO temperature loggers were intercalibrated against a PME miniDOT® optode (accuracy ±0.1°C) for 12 h under fluctuating temperatures (~18–45°C). Variability between loggers was <0.2°C.

Table 1. Sampling periods for temperature measurements conducted in the South Bay eelgrass meadow at the Virginia Coast Reserve Long-Term Ecological Research site (USA) in 2016–2020. Following a pilot study in 2016 (marked with *) we expanded our temperature network to 9 sites (see Fig. 1). Sampling periods were designed to capture summer temperatures in June–August of each year. We also report the total number of hours on record each year

Year	# sites	Deployment dates	Total # hours	Average # hours per site
2016*	7	20 Jun – 20 Aug	7983	1141
2017	15	26 May – 19 Oct	47259	3151
2018	15	31 May – 10 Sept	33920	2261
2019	15	14 May – 28 Oct	58148	3877
2020	15	1 Jun – 23 Aug	29785	1986

2.3. Eelgrass metrics

During summer 2019, eelgrass shoot density was counted within a 25 m radius of each temperature logger to capture spatial variation within the meadow. Eelgrass shoots were counted within 0.25 m^2 quadrats (n = 10) thrown haphazardly at each site, and we measured maximum shoot length as the length of the 3 longest leaves within each quadrat. These data were collected every 7–14 d from early July to mid-August. To capture variations in early-summer eelgrass biomass between the center and northern edge of the meadow (sites 4 and 0, respectively, Fig. 1), we also collected shoot density and length measurements once in May.

2.4. Heat stress patterns

Spatial and temporal patterns of temperature stress and relief in South Bay were evaluated based on the duration and magnitude of warming and cooling relative to the eelgrass ecosystem thermal tolerance threshold (T_{th} = 28.6°C, determined from >350 h of *in situ* eelgrass ecosystem metabolism measurements via aquatic eddy covariance; Berger & Berg 2024) at each site and during each summer. We cumulated the hourly water temperature anomalies above 28.6°C for each 24 h period in our temperature record (Fig. 2b). The resulting variable, daily heating degree-hours (HDHs), was calculated as:

$$\text{when } T_i > T_{th}\text{: } \mathrm{HDH} = \sum_{i=1}^{h} (T_i - T_{th}) \quad (1)$$

where T_{th} is the temperature threshold and T_i is the temperature at hour *i*. Daily HDHs were calculated for i = 1 to h = 24 (Table 2). Higher daily HDH values reflect more extreme water temperatures during the 24 h period (e.g. Fig. 2a,b). This metric was therefore used to identify the most prominent warming events each summer as successive days with elevated temperatures (high HDH values). Once these events were identified, we calculated the total HDHs as per Eq. (1) but for the entire duration of the heating event (e.g. Fig. 2c, Table 2). We then compared the severity of heating events between years by comparing mean HDHs per day (i.e. average daily heat stress during an event), calculated by dividing

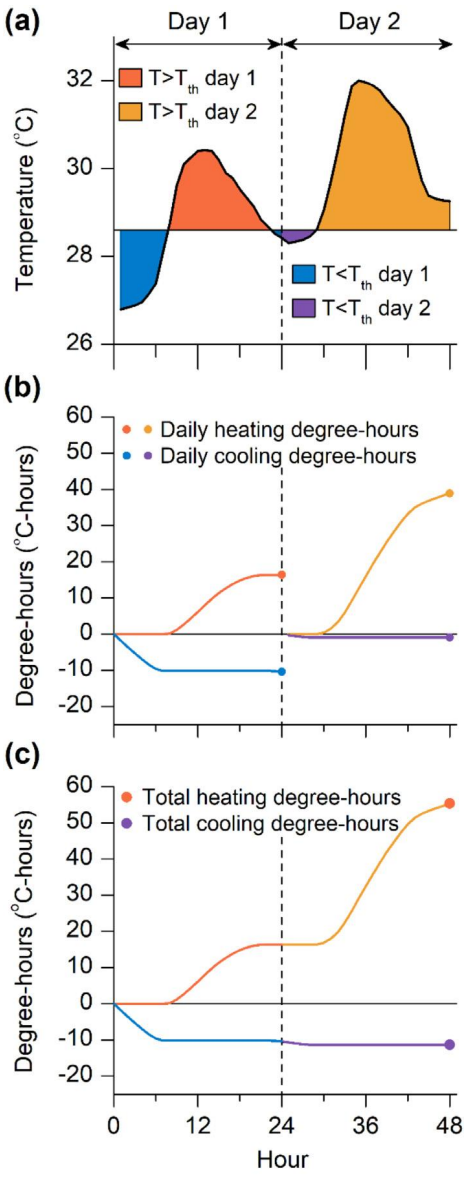

Fig. 2. Illustration of heat stress metrics used in this study. (a) Based on an hourly temperature record from site 0 (Fig. 1) on 12–13 July 2019, we identified the temperature anomalies above (warm colors) and below (cool colors) the local eelgrass ecosystem temperature stress threshold (T_{th}) of 28.6°C. (b) For each 24 h period, these temperature anomalies were cumulatively summed, resulting in daily heating and cooling degree-hours (daily HDHs and CDHs, respectively). (c) HDHs and CDHs were also cumulated over an entire heating event, illustrated here by 2 hot days, resulting in one value for heat stress (total HDHs) and one for heat stress relief (total CDHs)

total HDHs by the duration of the heating event (number of days, Table 2).

We took into account relief from heat stress during heating events by assessing spatiotemporal variations in the amount and duration of cooling (temperature < T_{th}) due to tidal input of cooler oceanic waters. We calculated total cooling degree-hours (CDHs, Table 2, Fig. 2) using Eq. (1) for $T_i < T_{th}$, as well as CDHs per day (CDH / n days):

$$\text{when } T_i < T_{th}\text{: } \text{CDH} = \sum_{i=1}^{h} (T_i - T_{th}) \quad (2)$$

Heat stress was related to spatiotemporal patterns in eelgrass shoot density and length during summer 2019 using simple linear regressions between eelgrass metrics (shoot density, shoot length) and heat stress metrics (mean HDHs and CDHs per day). Our small sample size (n = 5 sites, Fig. 1) prevented us from using a multivariate approach. The effects of heat stress on eelgrass growth during the summer were then assessed by comparing changes in shoot density during the natural meadow expansion and die-back periods at the center and northern sites (sites 0 and 4, respectively).

We also estimated the amount of heat stress necessary to cause an eelgrass die-off event similar to the one we observed in 2015. In 2015, eelgrass shoot density decreased by ~25% (from 316 to 230 shoots m^{-2}, Berg et al. 2019) between 27 April and 27 June — a period during which we would normally expect a significant increase (Orth & Moore 1986, Berger et al. 2020). This observed decrease in shoot density suggests the 2015 die-off (which ultimately resulted in a 90% loss of eelgrass) had started between these sampling dates. Because we had no *in situ* water temperature measurements in 2015, we used available data from the National Oceanic and Atmospheric Administration (NOAA) National Data Buoy Center for the nearby Wachapreague, VA (Stn WAHV2, ~39 km from South Bay). We first evaluated how well these records could serve as proxy for water temperatures at our main study site (center site, site 0, Fig. 1) by comparing the amount of heat stress (total HDHs) calculated from both the buoy and *in situ* temperature records for summer heating events when the datasets overlapped (2016–2020). We then used the Wachapreague temperature record to calculate heat stress from 27 April to 27 June 2015 and estimate the minimum total HDH value that could trigger an eelgrass die-off event, in comparison to the total HDHs from other years (2012–2014 and 2016–2020) where no decrease in shoot density was observed.

2.5. Sulfide presence in sediment and eelgrass tissue

To detect sulfide intrusion in eelgrass tissues as a possible contributor to the eelgrass die-off, we analyzed the sulfur isotopic signature of eelgrass leaf samples collected from biomass cores taken at the center

Table 2. Variables and definitions of the metrics used to quantify heat stress in this study

Variable name	Definition
HDH	Heating degree-hour (°C-hours): HDHs represent the amount of heating above a temperature threshold (T_{th}), calculated as the cumulative sum of hourly water temperature anomalies above T_{th}. High HDH values reflect more extreme heating in terms of duration and/or magnitude of high water temperatures
Daily HDHs	HDHs cumulated over each 24 h period
Total HDHs	HDHs cumulated over an entire heating event
Mean HDHs per day	To allow for better comparison of heating events between years, mean HDHs per day are calculated as total HDHs/n days during the heating event. They represent the average heat stress of a typical day during the event
CDH	Cooling degree-hour (°C-hours): CDHs represent the amount of cooling, or thermal stress relief, when temperatures drop below T_{th}, calculated as the cumulative sum of hourly water temperature anomalies below T_{th}. Higher absolute CDH values reflect longer and/or more extreme relief from thermal stress
Total CDHs	CDHs cumulated over an entire heating event
Mean CDHs per day	Similar to mean HDHs per day, mean CDHs per day represent the average thermal stress relief during a typical day during the event. Calculated as total CDHs/n days

site in June and/or July 2012–2019 (n = 3 cores per collection date, n = 33 cores total). Sediment samples were also collected in some years and were included in this analysis (n = 15 samples). These samples were collected adjacent to the eelgrass biomass cores using 5 cm deep and 2.5 cm wide cut-off syringe corers. Eelgrass leaves were rinsed, sorted, dried (at 60°C), and ground in preparation for the sulfur isotope analyses. Sediment samples were also dried and ground. All samples were analyzed at the Marine Biological Laboratory Stable Isotope Laboratory in Woods Hole, MA.

The sulfur isotopic signature ($\delta^{34}S$) of eelgrass leaf tissue indicates whether the leaves obtained their sulfur from sulfate ($\delta^{34}S \approx 21‰$) (Rees et al. 1978, Frederiksen et al. 2006) or toxic sulfide gas ($\delta^{34}S \approx 15–25‰$) (Canfield 2001, Böttcher et al. 2004). To assess whether there was sulfide intrusion during the die-off year (2015), we compared the $\delta^{34}S$ of eelgrass leaves and sediment ($\delta^{34}S_{eelgrass}$ and $\delta^{34}S_{sediment}$, respectively) between collection dates (data grouped by year and month, n = 11). We tested whether the mean $\delta^{34}S_{eelgrass}$ in July 2015 was considered an outlier in our record by performing Grubbs' test for detecting outliers (Grubbs 1950) using the 'outliers' package in R (version 3.4.2; R Core Team 2017).

Where we had both $\delta^{34}S_{eelgrass}$ and $\delta^{34}S_{sediment}$ for a given sampling date, we calculated the proportion of total sulfur in the plant coming from sulfide ($F_{sulfide}$) (Frederiksen et al. 2006) as:

$$F_{sulfide} = \frac{\delta^{34}S_{eelgrass} - \delta^{34}S_{sulfate}}{\delta^{34}S_{sediment} - \delta^{34}S_{sulfate}} \quad (3)$$

where $\delta^{34}S_{sulfate}$ is the sulfur isotopic signature of seawater. While this was not measured, $\delta^{34}S_{sulfate}$ values are fairly constant worldwide (Rees et al. 1978). We therefore used $\delta^{34}S_{sulfate} = 21‰$ to approximate $F_{sulfide}$ and evaluate relative changes in the contribution of sulfide to leaf sulfur in our record.

3. RESULTS

3.1. Spatiotemporal variations in temperature stress and eelgrass growth

For each of our summer water temperature datasets (2017–2020), we compared the temperature time series, daily HDHs, and total HDHs and CDHs over the most prominent heating events at the center and northern sites (Fig. 3, Table 3). Fig. 3a shows the temperature time series from 1 June to 31 August 2019 for both sites. Mean hourly summer temperature at the center site was significantly higher that of the northern site by 0.7°C (27.2 ± 0.05°C and 26.5 ± 0.05°C, respectively, n = 2208 hours, 2-sample *t*-test, $p < 0.01$). While the general variations over the summer agreed fairly well between the 2 sites as shown in Fig. 3, there were some time periods when temperatures at the northern site dropped well below those at the center site. For example, between 18 and 22 July, temperatures at the northern site dropped to ~25.5°C, while temperatures at the center site remained above the 28.6°C heat stress threshold, only dropping to ~30°C. Temperatures at the center site varied on a diel basis, whereas those at the northern site reflected a tidal cycle (Fig. 3a).

Periods of temperature stress in the eelgrass meadow each summer were identified using daily HDH values

(e.g. end of June through most of July 2019, Fig. 3b). The highest daily HDH values (i.e. the days of highest heat stress) occurred at the center site on 15 and 20 July 2019, with a cumulated 75 and 72°C-hours, respectively (Fig. 3b, Table 3). Heat stress at the northern site was ~60% lower on those days, with only

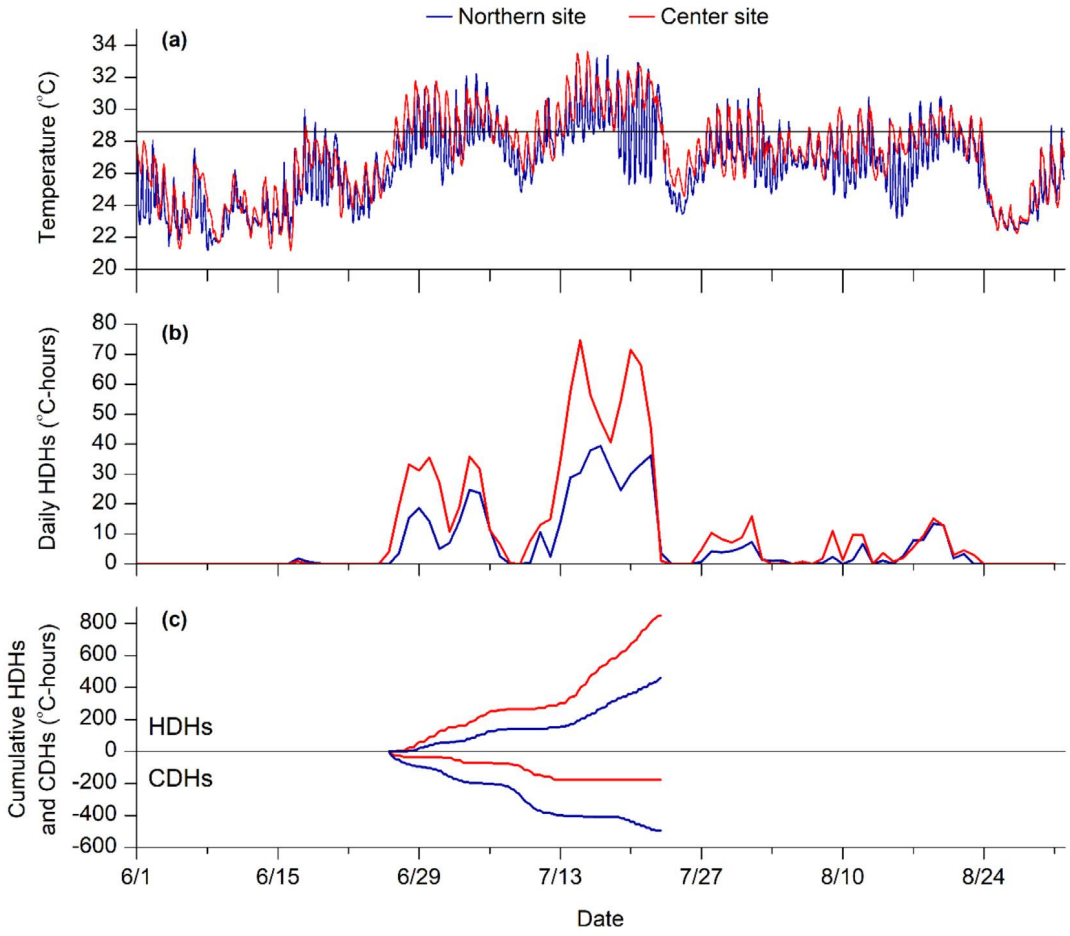

Fig. 3. Differences in temperature stress between the center and northern site in the meadow. (a) Hourly temperature time-series from 1 June to 31 August 2019 at the center site (red) and northern site (blue), relative to the 28.6°C temperature threshold (black line). (b) Daily heating degree-hours (HDHs) relative to 28.6°C at the center (red) and northern site (blue), and (c) cumulative HDHs and cooling degree-hours (CDHs) relative to 28.6°C at the center (red) and northern (blue) site during the warmest period of the summer

Table 3. Comparison of prominent warming events during summers 2017–2020 including event dates, duration (days), mean and maximum temperature (°C), maximum daily heating degree-hours (HDH,°C-hours), mean HDHs per day (°C-hours), and mean cooling degree-hours (CDHs) per day (°C-hours), for the northern and center sites. Dates are given as mo/d

Year	2017		2018		2019		2020	
Warmest period	7/2 – 7/23		6/19 – 7/7 and 8/5 – 8/31		6/26 – 7/22		6/28 – 7/30	
Duration	22		19, 27		27		29	
Site	Center	Northern	Center	Northern	Center	Northern	Center	Northern
Mean temperature	29.0	27.6	29.0, 28.4	28.4, 27.9	29.6	28.5	29.4	28.7
Max temperature	32.5	32.6	32.6, 32.7	32.7, 31.8	33.6	33.4	33.4	33.5
Max daily HDH	35	21	63, 38	45, 21	75	39	47	39
Mean HDH per day	19	9	25, 11	16, 8	31	17	30	14
Mean CDH per day	−10	−34	−15, −15	−19, −25	−7	−18	−5	−13

30°C-hours, peaking a few days later at 40°C-hours. Heating events in 2017–2020 lasted ~3–4 wk, but varied in intensity as can be seen in the daily HDH and mean HDH and CDH per day values in Table 3. The most intense warming periods occurred in 2019 and 2020. Each event lasted ~4 wk and had similarly high levels of heating (mean HDH per day = 30.5 and 15.5°C-hours at the center and northern sites, respectively) and low levels of cooling (mean CDH per day = −6 and −15.5°C-hours at the center and northern sites, respectively). Heating events in other years were less intense as they cumulated less heat (mean HDH per day values on average 56% lower) and more cooling (mean CDH per day values on average 60% higher) (Table 3).

Over the main hot period in 2019 (late June to late July, Fig. 3b), heat stress at the center site was 1.8 times higher than at the northern site (total HDH values of 850 and 460°C-hours, respectively) (Fig. 3c). The amount of cooling also differed strongly between the sites. Cooling at the northern site was 2.8 times greater than at the center site (−494 and −179°C-hours, respectively). Including all years on record (2017–2020), the center site experienced 1.4 to 2.1 (on average 1.8) times more heat stress than the northern site and received on average half (and as low as a third) the amount of thermal relief from temperatures below 28.6°C (Table 3).

Fig. 4 shows the differences in the amount of heating (mean HDH per day) and cooling (mean CDH per day) over all warm periods (2017–2020) between all sites along the north–south transect in the meadow. Maximum heating and minimum cooling occurred at site 1, one of the central sites (mean HDH per day = 19°C-hours) and decreased by 63% at the northern edge of the meadow (site 5). This decrease in heating was concurrent with a 64% increase in cooling between those sites. There was a similar trend in temperatures from the center of the meadow towards the southern inlet. Eelgrass metrics used as proxies for eelgrass growth in 2019 closely followed the observed heating and cooling trends (Fig. 4). Eelgrass shoot density and length generally increased from the center of the meadow northward as the amount of heating decreased and the amount of cooling increased (433 to 503 shoots m^{-2} and 45 to 66 cm, respectively). These relationships were all significant at the 0.1 level (linear regression p-values = 0.02–0.08 and adjusted R^2 = 0.6–0.8, n = 5, Table 4).

Fig. 5 shows how the difference in heat stress between the northern site (site 4, Fig. 4) and center site (site 0, Fig. 4) affected temporal eelgrass density patterns from early July to mid-August 2019. Over the last 10 d of the growing season, shoot densities increased substantially more at the northern site (43 vs. 7%). Subsequent decline rates, however, were comparable (47 vs. 37%).

3.2. Heat stress and eelgrass die-off events

The long-term Wachapreague buoy temperature records agreed well with the HOBO temperature data collected during this study at the center site that experienced the seagrass die-off. The total HDHs calculated during summer hot events during 2016–2020

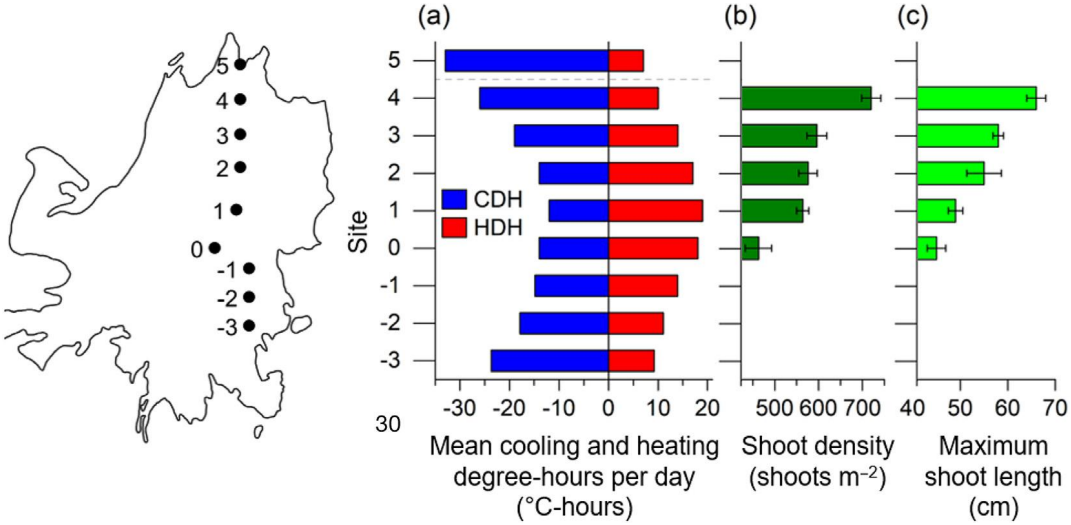

Fig. 4. Patterns of (a) heating, cooling, (b) eelgrass shoot density, and (c) maximum shoot length along a north–south transect in the meadow. Heating and cooling at each site were calculated as mean daily heating degree-hours (HDHs) (red) and cooling degree-hours (CDHs) (blue). Dashed grey line: meadow boundary. Error bars are ± SE (n = 20)

Table 4. Heating and cooling effects on eelgrass shoot density and length. Regression results (slope β, p-value, adjusted R^2) for simple linear regressions performed between heat stress metrics (heating: mean heating degree-hours per day; cooling: mean cooling degree-hours per day) and eelgrass metrics (shoot density in shoots m^{-2} and shoot length in cm) (n = 5)

	Heating	Cooling
Shoot density	β = −22 ± 7, p = 0.06, adj R^2 = 0.65	β = 14 ± 5, p = 0.08, adj R^2 = 0.60
Shoot length	β = −2.1 ± 0.5, p = 0.02, adj R^2 = 0.82	β = 1.3 ± 0.4, p = 0.04, adj R^2 = 0.74

were essentially identical between the 2 sites (Fig. 6a, R^2 = 1 and regression slope = 0.99, p < 0.01). Slightly greater variation was found for calculations between 27 April and 27 June 2018–2020 (Fig. 6b), with differences of 10–36°C-hours cumulated over the ~2 mo period when heating events were not targeted. Based on these results, temperature records from Wachapreague are an appropriate proxy for *in situ* temperatures at our center site when quantifying heat stress during warming events. We therefore used these records to quantify local heat stress during the June 2015 marine heatwave and found that warming between 27 April and 27 June 2015 was more prominent compared to that during the same period in other years (Fig. 6b). The heating event lasted for an uninterrupted 2 wk period, reaching maximum peak daily HDH of 33°C-hours and a total of 220°C-hours.

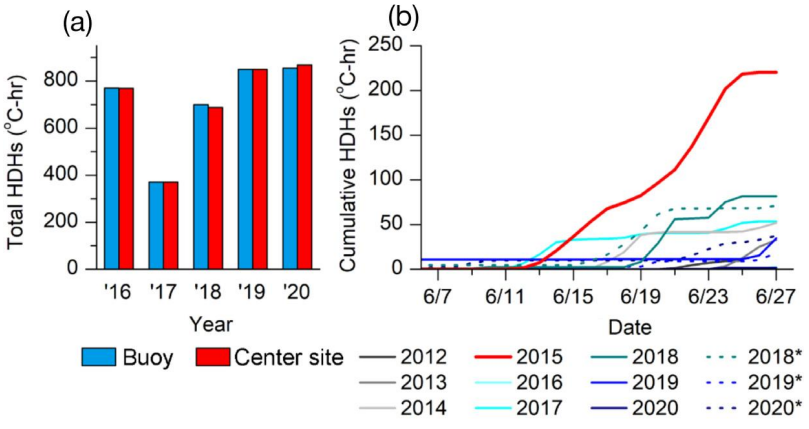

Fig. 6. (a) Comparison of heat stress (total heating degree-hours, HDHs) between temperature records from the center site and the National Data Buoy Center (NDBC) station WAHV2 during summer hot events in 2016–2020. (b) Unusually high heat stress (cumulative HDHs) in June 2015 compared to other years (2012–2016 buoy records and 2017–2020 *in situ* records). Asterisks (*) show cumulative HDHs calculated from matching buoy records

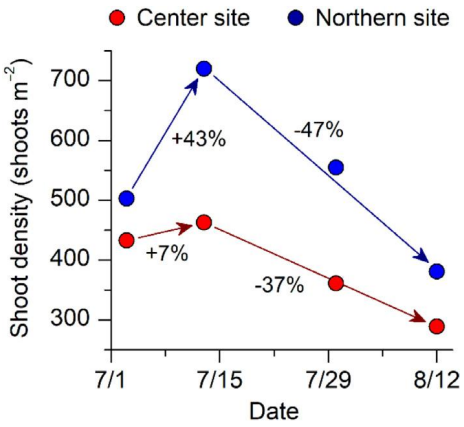

Fig. 5. Shoot densities at the center site (red) and northern site (blue) from 3 July to 12 August 2019. Numbers represent rates of increase and decline (in %) over the last week of the growing season and progression into late summer, respectively. Error bars (SE) are masked by symbols

In comparison, the total HDHs over this time period in the other years was nearly an order of magnitude lower, with an average of 33°C-hours. The year with the second highest amount of heat stress was 2018, which peaked at a daily HDH value of 27°C-hours and totaled at 82°C-hours (Fig. 6b).

3.3. Sediment temperatures

Temperatures in the sediment were strongly linked to water column temperatures. Fig. 7 shows the temperature time series at the northern and center sites from 6–13 August 2018 in the water column, and 2.5 and 5 cm deep in the sediment. While no temperature stratification occurred in the water column, temperature fluctuations were attenuated from the water column to 2.5 and 5 cm deep in the sediment (ANOVAs: $F_{2,1434}$ = 20 and 22 for the center and northern sites, respectively, p < 0.05; Fig. 7). Average temperature attenuations were almost negligible, yet statistically significant (2-sample *t*-tests, p > 0.05), with an average decrease of 0.3°C between the water column and 2.5 cm into the sediment, and 0.2°C between 2.5 and 5 cm deep in the sediment. The largest temperature differences between the water column and sediment were found in peak temperatures during the day (repeated measures ANOVAs: $F_{1,18}$ = 148 and $F_{1,30}$ = 209 for the center and northern site, respectively, p < 0.05), which

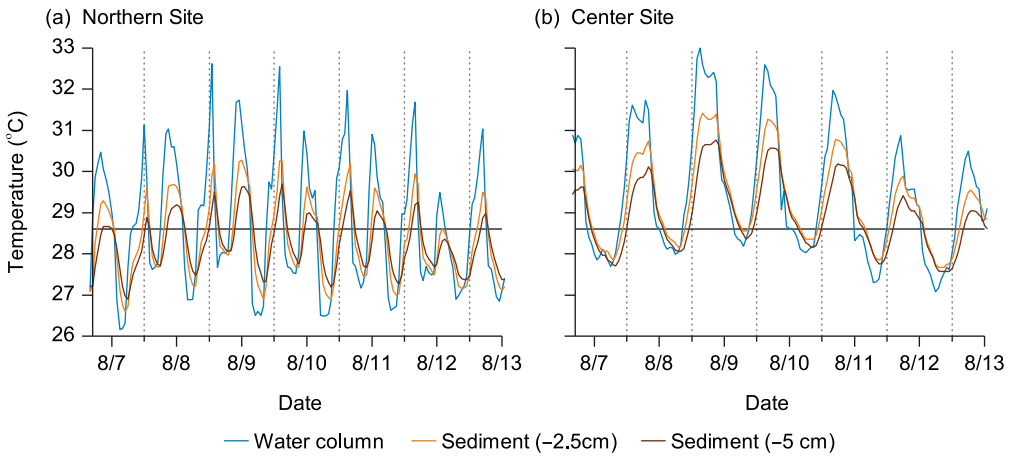

Fig. 7. Temperature attenuation in the sediment compared to the water column at the (a) northern and (b) center site. Hourly temperatures from 6–13 August 2018 in the water column (blue) and in the root zone, 2.5 cm (orange) and 5 cm (red) into the sediment. Dashed grey lines represent midday (12:00 h)

were on average 1°C warmer in the water column than 2.5 cm deep in the sediment, and 1.5°C warmer than 5 cm deep in the sediment (all statistically significant differences, 2-sample *t*-tests, $p < 0.05$). Differences in minimum temperatures between the water column and sediment were smaller. On average, minimum temperatures in the water column were 0.4°C cooler than in the sediment (non-significant, 2-sample *t*-tests, $p > 0.1$).

3.4. Sulfide

The sulfur isotopic signatures ($\delta^{34}S$) of leaf samples from June and/or July 2012–2019 are shown in Fig. 8. The $\delta^{34}S$ of samples taken outside of 2015 averaged 13.9 ± 1.5‰ (±SD, n = 9). From June to July 2015, however, the $\delta^{34}S$ of eelgrass tissues dropped from 13.5 ± 0.7 to 8.4 ± 0.5‰ (a value identified as a statistical outlier in our 7 yr record: Grubbs' test, $p < 0.05$, n = 11), coincident with the eelgrass die-off due to heat stress. The $F_{sulfide}$ values calculated from eelgrass and sediment $\delta^{34}S$ values showed a higher contribution of sulfide to plant sulfur in July 2015 compared to any of the previous or subsequent years (34 vs. 16–25%, respectively).

4. DISCUSSION

Identifying marine heatwaves and other extreme temperature events and properly quantifying heat stress are key to forecasting changes in marine ecosystems induced by climate change. This study quantified the duration and intensity of heat stress based on extensive local water column temperature measurements and a known eelgrass ecosystem heat tolerance threshold derived from aquatic eddy covariance measurements at the same site. Here, we propose the first heat stress metrics linked to the ecological response of an eelgrass meadow that include both heating and cooling effects.

We found that both the timing of heating events in eelgrass meadows and their spatial location with respect to cooling modulated the ecological impacts of extreme warming, and that heat stress at the scale of hours to days can strongly impact eelgrass density. The initiation of heat stress during the early growing season, with the possible added effects of sulfide toxicity, triggered the eelgrass mortality event we observed in 2015. The impact of the heatwave depended

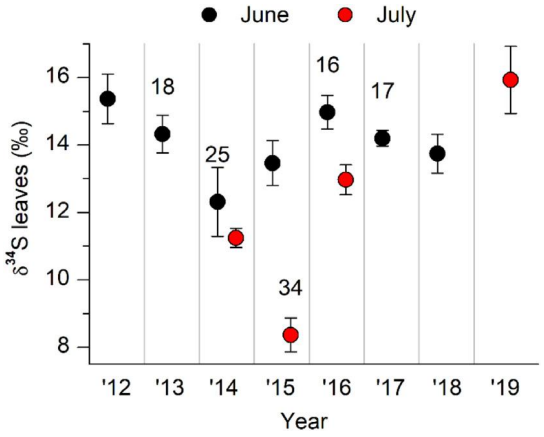

Fig. 8. Timeseries of the $\delta^{34}S$ of eelgrass leaves collected in June (black) and/or July (red) of each year from 2012 to 2019. Numbers represent the proportion of sulfur in the eelgrass tissue coming from sediment sulfide ($F_{sulfide}$, expressed as a percentage). Error bars are ± SE

on spatial location within the meadow, with sites farthest from the ocean inlet experiencing less cooling during incoming tides and greater heat stress, which resulted in lower shoot density and canopy height.

This study advances our understanding of seagrass meadow response to heat stress, and improves our ability to quantify the intensity and duration of both heating and cooling. Defining metrics for monitoring heating and cooling that impact seagrass biomass lays the groundwork for forecasting seagrass meadow vulnerability and resilience to future warming oceans and more frequent temperature extremes.

4.1. Heat stress metrics

Increased ocean temperatures and more frequent severe heating events are impacting seagrass meadows globally (e.g. Thomson et al. 2015, Arias-Ortiz et al. 2018, Berger et al. 2020), yet we lack appropriate measures to quantify heat stress that can help manage seagrass ecosystems in the face of climate change. The 2 most common metrics are based on climatological thresholds: marine heatwaves are defined based on the 90th percentile of mean SSTs (Hobday et al. 2016), and degree heating weeks are defined based on mean monthly maximum SSTs (Liu et al. 2014). Both of these rely on long-term records of SSTs and are valuable in identifying periods of unusually high temperatures. However, they do not take relief from heat stress into consideration and are sometimes deemed insufficient as sole metrics for explaining different degrees of seagrass loss. For example, Strydom et al. (2020) found that degree heating weeks alone could only explain ~22% of observed spatial variations in seagrass loss in Australia. We argue that heat stress calculations need to be based both on the inherent vulnerability of a species or ecosystem to temperature stress (i.e. temperature threshold), and the duration and intensity of both heating and cooling on hourly time scales. Previous studies in other locations have shown both plasticity and adaptation of eelgrass to local temperatures, and so determination of temperature thresholds should be both species- and location-specific (Reynolds et al. 2016, Duarte et al. 2018, DuBois et al. 2020). The contribution of different community components may vary across locations, so it is important to establish system-specific temperature thresholds, as these different components may respond differently to increasing temperatures (Murray & Wetzel 1987).

In this study, we used the temperature tolerance threshold of 28.6°C for the eelgrass meadow in our study system, which we determined from a decade of *in situ* aquatic eddy covariance measurements of eelgrass ecosystem metabolism (Berger & Berg 2024). In comparison, the thresholds for defining marine heatwaves at the VCR were determined based on 24 yr temperature records to be on average 27.6°C in June and 29.4°C in July (Aoki et al. 2021). Due to the mismatch between the climatological thresholds and the physiological heat stress temperature threshold for this eelgrass ecosystem, heating events that cause negative ecological impacts may or may not meet the definition of a marine heatwave. Furthermore, we have demonstrated that hourly-scale heating and cooling influence the ecological impact of heating events on eelgrass meadows, whereas marine heatwaves require the temperature to remain elevated above the climatological threshold for at least 5 successive days. The climatological definitions aid in comparing marine heatwave events through time and space, but they do not fully capture the ecological impacts of warming oceans. For seagrass ecosystems, more specific metrics that capture finer temporal variations in temperature, such as the HDHs and CDHs defined here, are needed to identify and evaluate heat stress impacts.

These novel metrics allowed us to compare the intensity of heat stress between sites within the same meadow (Fig. 4), thus providing a more refined picture of heat stress dynamics at smaller spatial scales (~200 m) compared to the coarser resolution of satellite-derived SST images (e.g. 1 km^2). HDHs were also useful in comparing heating events between years, particularly events of similar duration but contrasting intensity (Table 3), and mean HDHs per day were useful in comparing the cumulated heat stress over heating events of different lengths. For example, both 2018 and 2019 had a 27 d warm period. However, the 2018 event was about half as intense as the 2019 event, with peak HDH values at the center site of 38°C-hours (2018) and 75°C-hours (2019), and mean HDHs per day of 11°C-hours (2018) and 31°C-hours (2019) (Table 3). Comparing daily HDHs enabled us to identify the most intense periods of heat stress in the temperature record, which might have been missed had we only used average weekly temperatures (Fig. 3).

The inclusion of cooling effects in our metrics (CDHs) also provided more information about daily temperature conditions where periodic cooling can provide relief from cumulative heat stress. Our analysis showed that neighboring sites within the same meadow can experience contrasting patterns of heating and cooling (Figs. 3 & 4). The tidally-driven north-

ern site (site 4) often exhibited more extreme temperature fluctuations throughout the day, with periods of high temperatures followed by cooler periods of relief driven by the input of colder ocean water during flood tides (Figs. 3 & 7). In contrast, the center site (site 0), which experienced nearly double the heat stress, exhibited less extreme temperature fluctuations, as seen in the lower (2–3×) CDHs, which indicate less stress relief and therefore less tidal influence. Krumhansl et al. (2021) similarly showed that seagrass sites with less water flow were warmer, exhibited less temperature variability, and had lower productivity and resilience. CDHs would also be a useful differentiator between sites that may have the same cumulative HDHs over the duration of a heating event, but different temperature profiles. In comparison to our northern site described above, which experiences short pulses of high temperatures followed by cooler periods of heat stress relief, another hypothetical site could have the same total HDH value at the end of a heating event, without having experienced any relief from heat stress. This site would have experienced less extreme temperatures relative to T_{th}, but the heat stress experienced would be more persistent rather than intermittent. Our work therefore suggests that it is critically important to include both the cumulative heating and cooling relative to a temperature threshold in future studies to tease out the effects of ocean warming on coastal marine ecosystems.

4.2. Heat stress effects on eelgrass biomass

Shoot densities and lengths were ~65% higher at sites that experienced less heating and more cooling (with a mean HDH per day to CDH per day ratio of 0.4) compared to sites at the more heat-stressed center of the meadow (mean ratio of HDH to CDH = 1.4 for the 3 most stressed sites, Fig. 4). Our results document a general trend of more thriving eelgrass at sites that benefit from proximity to the ocean inlet and more pronounced tidal cooling (Fig. 1). These findings agree with those of Moore et al. (2012), who found higher eelgrass expansion in meadows that experienced tidal cooling. Including more sites in future studies could help tease out the relative importance of HDH and CDH in driving patterns of eelgrass shoot density and length. The effects of tidal cooling are also evident in the differences in shoot density change between the center and northern sites during the growing season (7 and 43% increases, respectively, Fig. 5). This difference between the 2 sites (36%) is much larger than the difference in meadow thinning at the end of the growing season in late summer (10%). This suggests that heat stress plays a more important role in eelgrass expansion during the growing season, as opposed to the late summer during natural eelgrass senescence. This is further supported by the observed decline in eelgrass shoot density between 27 April and 27 June 2015 (Berg et al. 2019), a period during which heat stress was considerable (Fig. 6b).

4.3. Role of co-stressors

While high water temperatures are recognized as a main driver of eelgrass die-off events (e.g. Marbá & Duarte 2010, Arias-Ortiz et al. 2018, Berger et al. 2020, Aoki et al. 2021), our results suggest sulfide toxicity may have also contributed to the eelgrass mortality we observed in 2015 (Fig. 8). Multiple studies have previously connected seagrass mortality to the combined effects of high water temperatures and sulfide intrusion (Greve et al. 2003, Borum et al. 2005, Holmer & Hasler-Sheetal 2014), despite sulfide intrusion alone not always driving seagrass declines (Moksnes et al. 2018). Elevated temperatures cause an increase in oxygen demand from seagrass tissues, which — combined with potentially low oxygen availability (e.g. during ecosystem respiration at night and/or during slack tide in dense canopies) — may lead tissues to become hypoxic and thus susceptible to sulfide intrusion (Greve et al. 2003). Our results indeed suggest a higher proportion of sulfide intake by eelgrass leaves in 2015 compared to other years ($F_{sulfide}$ = 25 and 34% in 2014 and 2015, respectively, Fig. 8). McGlathery (2018) showed a higher proportion of dead eelgrass biomass just after the die-off even started in June 2015 (above and belowground dead:live biomass ratio = 1.4) compared to early summer ratios consistently <1 in other years (on average 0.7 for 2014, 2016, and 2017, n = 7). Based on our findings that, while dampened, temperature fluctuations in the sediment followed those of the water column and could reach similarly high temperatures (>28.6°C, Fig. 7), we suspect the initial warming in June 2015 led to increased respiration rates in the sediment which, combined with newly added organic matter from the onset of the die-off event, led to higher sulfide concentrations in the sediment. Coupled with the weakened resistance to sulfide intrusion of heat-stressed eelgrass, we consider it likely that sulfide toxicity exacerbated the eelgrass decline. However, it is also possible that the eelgrass in the meadow interior was already more sensitive to heat stress if some sulfide intrusion was

already occurring (Goodman et al. 1995) as a result of higher sediment organic matter content (2.6–3%) — and therefore higher sulfide production — compared to sites closer to the edges of the meadow (1–1.4%) (Oreska et al. 2017). This highlights the need to consider synergistic feedbacks between co-stressors when assessing future impacts of marine heating on seagrass ecosystems (Lefcheck et al. 2017). The combined effects of 2 stressors — in this case high temperatures and sulfide toxicity — likely had a stronger negative effect on eelgrass survival compared to exposure to heat stress only (Moreno-Marín et al. 2018). While light availability has generally not been considered a stressor in the coastal lagoons at the VCR (Lawson et al. 2007, Moore et al. 2012), it is possible that the increased windiness (Juska & Berg 2022) and precipitation in this region (Najjar et al. 2000, Polsky et al. 2000) will result in light availability becoming a more important stressor, as it is in other nearby areas (e.g. Moore & Jarvis 2008, Moore et al. 2014). Sulfide intrusion and high temperatures both negatively impact seagrass photosynthesis and increase light requirements to remain productive (e.g. Marsh et al. 1986, Goodman et al. 1995, Moore et al. 1997, Lee et al. 2007, Staehr & Borum 2011, Ewers 2013, Kim et al. 2020). The added effects of reduced light availability on this decreased photosynthetic efficiency would exacerbate the negative impacts of temperature and/or sulfide intrusion on eelgrass growth and survival. This should be taken into account in future studies.

4.4. High temperature-induced die-off events

Because of the close match between the amount of heat stress calculated for summer heating events at the Wachapreague station and at our center site, we were confident in using the Wachapreague buoy record from 2015 to accurately estimate the amount of heat stress that initiated the die-off event (Fig. 6a). Given the small-scale (<1 km) differences in heat stress within South Bay, this record could not have been used to directly estimate HDH at another site in the meadow. This highlights the challenge of using non-site data as a proxy for *in situ* conditions, and we recommend deploying temperature loggers (HOBO Pendant® temperature loggers are relatively inexpensive) in areas of interest for continuous monitoring or to derive relationships between *in situ* data and more publicly available long-term records.

Heating in June 2015 lasted much longer (~2 wk) and reached a higher daily HDH than early summer heating in other years. It also cumulated a total of 220°C-hours, more than 2.5 times the amount cumulated in the second hottest June (82°C-hours in 2018, Fig. 6b). These results suggest that the amount of heat stress during the growing season capable of triggering an eelgrass die-off event is likely to fall in the range of ~100–200°C-hours. Although this estimate is broad, it provides a first baseline for determining the suitability of potential restoration sites in this region, and for predicting future changes in eelgrass cover under future ocean warming scenarios.

Future increases in the frequency and severity of high-temperature events (including marine heatwaves) may present a challenge for the resilience of seagrass meadows and their ecosystem services (Duarte et al. 2020). While there is evidence of seagrass adaptability and plasticity in response to marine heatwaves that could mediate resilience to subsequent heat stress, it is still unclear whether these processes will keep up with global change and whether they last interannually and intergenerationally (Reynolds et al. 2016, DuBois et al. 2020, Jueterbock et al. 2020, Nguyen et al. 2020). Jueterbock et al. (2020) and Nguyen et al. (2020) have shown that the molecular changes associated with the seagrass metabolic response to heat stress can be memorized for several weeks after a heating event and thus confer greater resilience to subsequent events. This may explain why the timing of heating events matters, and why an early-summer marine heatwave in 2015 caused such a pronounced eelgrass decline, compared to marine heatwaves in July that were not associated with eelgrass loss (Table 3, Berger et al. 2020). In addition to this, spring and early summer represent the peak growing season for eelgrass (Orth & Moore 1986), with peak production (Berger et al. 2020) and accumulation of non-structural carbohydrate reserves (Burke et al. 1996). These reserves are necessary for the plants to survive periods of reduced net photosynthesis during stressful summer conditions and the fall and winter (Burke et al. 1996). Unusual heat stress during this critical period could cause the plants to deplete the reserves they would need to last through the heating event or the rest of the summer, which would lead to biomass loss. This explanation was also proposed by Moore et al. (2014) and Shields et al. (2019) after 2 early-season heating events in 2010 and 2015 caused eelgrass losses in the Chesapeake Bay.

Future ocean warming and increasingly frequent marine heatwaves underscore the need for a full understanding of heatwave impacts on seagrass ecosystems to better characterize seagrass habitat suit-

ability in a changing climate. This includes understanding the inherent ecosystem vulnerability to heat stress (T_{th}) and the variability of both heating and cooling effects. Additional research is needed to understand how the timing and seasonality of heating events contribute to seagrass decline, including the effects of winter warming, which can also deplete seagrass energy reserves, leading to early flowering and spring mortality (Sawall et al. 2021).

Acknowledgements. This work was supported by the National Science Foundation (Virginia Coast Reserve Long Term Ecological Research grant, DEB-1237733 and DEB-1832221). We thank the staff at the University of Virginia's Anheuser-Busch Coastal Research Center for their field and lab assistance, as well as S. Cox and other REU students for their help in data collection.

LITERATURE CITED

Aoki LR, McGlathery KJ, Oreska MPJ (2020a) Seagrass restoration reestablishes the coastal nitrogen filter through enhanced burial. Limnol Oceanogr 65:1–12

Aoki LR, McGlathery KJ, Wiberg PL, Al-Haj A (2020b) Depth affects seagrass restoration success and resilience to marine heat wave disturbance. Estuar Coasts 43:316–328

Aoki LR, McGlathery KJ, Wiberg PL, Oreska MPJ, Berger AC, Berg P, Orth RJ (2021) Seagrass recovery following marine heat wave influences sediment carbon stocks. Front Mar Sci 7:576784

Arias-Ortiz A, Serrano O, Masqué P, Lavery PS and others (2018) A marine heatwave drives massive losses from the world's largest seagrass carbon stocks. Nat Clim Change 8:338–344

Armitage AR, Fourqurean JW (2016) Carbon storage in seagrass soils: Long-term nutrient history exceeds the effects of near-term nutrient enrichment. Biogeosciences 13:313–321

Berg P, Delgard ML, Polsenaere P, McGlathery KJ, Doney SC, Berger AC (2019) Dynamics of benthic metabolism, O_2, and pCO_2 in a temperate seagrass meadow. Limnol Oceanogr 64:2586–2604

Berger AC, Berg P (2024) Eelgrass meadow response to heat stress. I. Temperature threshold for ecosystem production derived from *in situ* aquatic eddy covariance measurements. Mar Ecol Prog Ser 736:35–46

Berger AC, Berg P, McGlathery KJ, Delgard ML (2020) Long-term trends and resilience of seagrass metabolism: a decadal aquatic eddy covariance study. Limnol Oceanogr 65:1423–1438

Borum J, Pedersen O, Greve TM, Frankovich TA, Zieman JC, Fourqurean JW, Madden CJ (2005) The potential role of plant oxygen and sulphide dynamics in die-off events of the tropical seagrass, *Thalassia testudinum.* J Ecol 93: 148–158

Böttcher ME, Khim BK, Suzuki A, Gehre M, Wortmann UG, Brumsack HJ (2004) Microbial sulfate reduction in deep sediments of the Southwest Pacific (ODP Leg 181, Sites 1119–1125): evidence from stable sulfur isotope fractionation and pore water modeling. Mar Geol 205:249–260

Burke MK, Dennison WC, Moore KA (1996) Non-structural carbohydrate reserves of eelgrass *Zostera marina.* Mar Ecol Prog Ser 137:195–201

Calleja ML, Marbá N, Duarte CM (2007) The relationship between seagrass (*Posidonia oceanica*) decline and sulfide porewater concentration in carbonate sediments. Estuar Coast Shelf Sci 73:583–588

Canfield DE (2001) Biogeochemistry of sulfur isotopes. Rev Mineral Geochem 43:607–636

Collier CJ, Uthicke S, Waycott M (2011) Thermal tolerance of two seagrass species at contrasting light levels: implications for future distribution in the Great Barrier Reef. Limnol Oceanogr 56:2200–2210

Costanza R, d'Arge R, De Groot R, Farber S and others (1997) The value of the world's ecosystem services and natural capital. Nature 387:253–260

Duarte B, Martins I, Rosa R, Matos AR and others (2018) Climate change impacts on seagrass meadows and macroalgal forests: an integrative perspective on acclimation and adaptation potential. Front Mar Sci 5:190

Duarte GAS, Villela HDM, Deocleciano M, Silva D and others (2020) Heat waves are a major threat to turbid coral reefs in Brazil. Front Mar Sci 7:179

DuBois K, Williams SL, Stachowicz JJ (2020) Previous exposure mediates the response of eelgrass to future warming via clonal transgenerational plasticity. Ecology 101: e03169

Ewers CJ (2013) Assessing physiological thresholds for eelgrass (*Zostera marina* L.) survival in the face of climate change. MSc thesis, California Polytechnic State University, San Luis Obispo, CA

Fagherazzi S, Wiberg PL (2009) Importance of wind conditions, fetch, and water levels on wave-generated shear stresses in shallow intertidal basins. J Geophys Res 114: F03022

Fourqurean JW, Duarte CM, Kennedy HA, Marbà N and others (2012) Seagrass ecosystems as a globally significant carbon stock. Nat Geosci 5:505–509

Frederiksen MS, Glud RN (2006) Oxygen dynamics in the rhizosphere of *Zostera marina*: a two-dimensional planar optode study. Limnol Oceanogr 51:1072–1083

Frederiksen MS, Holmer M, Borum J, Kennedy HA (2006) Temporal and spatial variation of sulfide invasion in eelgrass (*Zostera marina*) as reflected by its sulfur isotopic composition. Limnol Oceanogr 51:2308–2318

Frölicher TL, Fischer EM, Gruber N (2018) Marine heatwaves under global warming. Nature 560:360–364

Goodman JL, Moore KA, Dennison WC (1995) Photosynthetic responses of eelgrass (*Zostera marina* L) to light and sediment sulfide in a shallow barrier-island lagoon. Aquat Bot 50:37–47

Greve TM, Borum J, Pedersen O (2003) Meristematic oxygen variability in eelgrass (*Zostera marina*). Limnol Oceanogr 48:210–216

Grubbs FE (1950) Sample criteria for testing outlying observations. Ann Math Stat 21:27–58

Hobday AJ, Alexander LV, Perkins SE, Smale DA and others (2016) A hierarchical approach to defining marine heatwaves. Prog Oceanogr 141:227–238

Holmer M, Hasler-Sheetal H (2014) Sulfide intrusion in seagrasses assessed by stable sulfur isotopes – a synthesis of current results. Front Mar Sci 1:64

Holmer M, Nielsen SL (1997) Sediment sulfur dynamics related to biomass-density patterns in *Zostera marina* (eelgrass) beds. Mar Ecol Prog Ser 146:163–171

Hughes TP, Kerry JT, Álvarez-Noriega M, Álvarez-Romero

JG and others (2017) Global warming and recurrent mass bleaching of corals. Nature 543:373–377
Jueterbock A, Boström C, Coyer JA, Olsen JL and others (2020) The seagrass methylome memorizes heat stress and is associated with variation in stress performance among clonal shoots. Front Plant Sci 11:571646
Juska I, Berg P (2022) Variation in seagrass meadow respiration measured by aquatic eddy covariance. Limnol Oceanogr Lett 7:410–418
Kim M, Qin LZ, Kim SH, Song HJ, Kim YK, Lee KS (2020) Influence of water temperature anomalies on the growth of *Zostera marina* plants held under high and low irradiance levels. Estuar Coasts 43:463–476
Koch EW, Barbier EB, Silliman BR, Reed DJ and others (2009) Non-linearity in ecosystem services: temporal and spatial variability in coastal protection. Front Ecol Environ 7:29–37
Krumhansl KA, Dowd M, Wong MC (2021) Multiple metrics of temperature, light, and water motion drive gradients in eelgrass productivity and resilience. Front Mar Sci 8: 597707
Lawson SE, Wiberg PL, McGlathery KJ, Fugate DC (2007) Wind-driven sediment suspension controls light availability in a shallow coastal lagoon. Estuar Coasts 30: 102–112
Lawson SE, McGlathery KJ, Wiberg PL (2012) Enhancement of sediment suspension and nutrient flux by benthic macrophytes at low biomass. Mar Ecol Prog Ser 448:259–270
Lee KS, Park SR, Kim YK (2007) Effects of irradiance, temperature, and nutrients on growth dynamics of seagrasses: a review. J Exp Mar Biol Ecol 350:144–175
Lefcheck JS, Wilcox DJ, Murphy RR, Marion SR, Orth RJ (2017) Multiple stressors threaten the imperiled coastal foundation species eelgrass (*Zostera marina*) in Chesapeake Bay, USA. Glob Change Biol 23:3474–3483
Liu G, Heron SF, Eakin CM, Muller-Karger FE and others (2014) Reef-scale thermal stress monitoring of coral ecosystems: new 5-km global products from NOAA Coral Reef Watch. Remote Sens 6:11579–11606
Macreadie PI, Anton A, Raven JA, Beaumont N and others (2019) The future of Blue Carbon science. Nat Commun 10:3998
Marbà N, Duarte CM (2010) Mediterranean warming triggers seagrass (*Posidonia oceanica*) shoot mortality. Glob Change Biol 16:2366–2375
Marsh JA Jr, Dennison WC, Alberte RS (1986) Effects of temperature on photosynthesis and respiration in eelgrass (*Zostera marina* L.). J Exp Mar Biol Ecol 101:257–267
Mateo MÁ, Sánchez-Lizaso JL, Romero J (2003) *Posidonia oceanica* 'banquettes': a preliminary assessment of the relevance for meadow carbon and nutrients budget. Estuar Coast Shelf Sci 56:85–90
McGlathery KJ (2018) Above- and below-ground biomass and canopy height of seagrass in Hog Island Bay and South Bay, VA 2007–2017 ver 17. Environmental Data Initiative. https://doi.org/10.6073/pasta/09a0ce35bb3fc72113b5a16ad5b0d6bd
Moksnes PO, Eriander L, Infantes E, Holmer M (2018) Local regime shifts prevent natural recovery and restoration of lost eelgrass beds along the Swedish West Coast. Estuar Coasts 41:1712–1731
Moore KA, Jarvis JC (2008) Eelgrass diebacks in the lower Chesapeake Bay: implications for long-term persistence. J Coast Res 2008:135–147
Moore KA, Short FT (2006) *Zostera*: biology, ecology, and management. In: Larkum R, Orth RJ, Duarte CM (eds) Seagrasses: biology, ecology and conservation. Springer, Dordrecht, p 361–386
Moore KA, Wetzel RL, Orth RJ (1997) Seasonal pulses of turbidity and their relations to eelgrass (*Zostera marina* L.) survival in an estuary. J Exp Mar Biol Ecol 215:115–134
Moore KA, Shields EC, Parrish DB, Orth RJ (2012) Eelgrass survival in two contrasting systems: role of turbidity and summer water temperatures. Mar Ecol Prog Ser 448: 247–258
Moore KA, Shields EC, Parrish DB (2014) Impacts of varying estuarine temperature and light conditions on *Zostera marina* (eelgrass) and its interactions with *Ruppia maritima* (widgeongrass). Estuar Coasts 37:20–30
Moreno-Marín F, Brun FG, Pedersen MF (2018) Additive response to multiple environmental stressors in the seagrass *Zostera marina* L. Limnol Oceanogr 63:1528–1544
Murray L, Wetzel RL (1987) Oxygen production and consumption associated with the major autotrophic components in two temperate seagrass communities. Mar Ecol Prog Ser 38:231–239
Nagelkerken I, van der Velde G, Gorissen MW, Meijer GJ, Van't Hof T, den Hartog C (2000) Importance of mangroves, seagrass beds and the shallow coral reef as a nursery for important coral reef fishes, using a visual census technique. Estuar Coast Shelf Sci 51:31–44
Najjar RG, Walker HA, Anderson PJ, Barron EJ and others (2000) The potential impacts of climate change on the mid-Atlantic coastal region. Clim Res 14:219–233
Nguyen HM, Kim M, Ralph PJ, Marín-Guirao L, Pernice M, Procaccini G (2020) Stress memory in seagrasses: first insight into the effects of thermal priming and the role of epigenetic modifications. Front Plant Sci 11:494
Oliver ECJ, Burrows MT, Donat MG, Sen Gupta A and others (2019) Projected marine heatwaves in the 21st century and the potential for ecological impact. Front Mar Sci 6:734
Oreska MPJ, McGlathery KJ, Porter JH, Asmus H, Asmus RM, Vaquer A (2017) Seagrass blue carbon spatial patterns at the meadow-scale. PLOS ONE 12:e0176630
Oreska MPJ, McGlathery KJ, Wiberg PL, Orth RJ, Wilcox DJ (2021) Defining the *Zostera marina* (eelgrass) niche from long-term success of restored and naturally colonized meadows: implications for seagrass restoration. Estuar Coasts 44:396–411
Orth RJ, McGlathery KJ (2012) Eelgrass recovery in the coastal bays of the Virginia Coast Reserve, USA. Mar Ecol Prog Ser 448:173–176
Orth RJ, Moore KA (1986) Seasonal and year-to year variations in the growth of *Zostera marina* L. (eelgrass) in the lower Chesapeake Bay. Aquat Bot 24:335–341
Orth RJ, Luckenbach ML, Marion SR, Moore KA, Wilcox DJ (2006) Seagrass recovery in the Delmarva Coastal Bays, USA. Aquat Bot 84:26–36
Orth RJ, Lefcheck JS, McGlathery KS, Aoki LR and others (2020) Restoration of seagrass habitat leads to rapid recovery of coastal ecosystem services. Sci Adv 6: eabc6434
Pedersen O, Binzer T, Borum J (2004) Sulphide intrusion in eelgrass (*Zostera marina* L.). Plant Cell Environ 27: 595–602
Pendleton L, Donato DC, Murray BC, Crooks S and others (2012) Estimating global 'blue carbon' emissions from conversion and degradation of vegetated coastal ecosystems. PLOS ONE 7:e43542

Polsky C, Allard J, Currit N, Crane R, Yarnal B (2000) The Mid-Atlantic region and its climate: past, present, and future. Clim Res 14:161–173

R Core Team (2017) R: a language and environment for statistical computing. R Foundation for Statistical Computing, Vienna

Rees CE, Jenkins WJ, Monster J (1978) The sulphur isotopic composition of ocean water sulphate. Geochim Cosmochim Acta 42:377–381

Rees SE, Rodwell LD, Attrill MJ, Austen MC, Mangi SC (2010) The value of marine biodiversity to the leisure and recreation industry and its application to marine spatial planning. Mar Policy 34:868–875

Reynolds LK, DuBois K, Abbott JM, Williams SL, Stachowicz JJ (2016) Response of a habitat-forming marine plant to a simulated warming event is delayed, genotype specific, and varies with phenology. PLOS ONE 11: e0154532

Sawall Y, Ito M, Pansch C (2021) Chronically elevated sea surface temperatures revealed high susceptibility of the eelgrass *Zostera marina* to winter and spring warming. Limnol Oceanogr 66:4112–4124

Shields EC, Parrish D, Moore KA (2019) Short-term temperature stress results in seagrass community shift in a temperate estuary. Estuar Coasts 42:755–764

Skirving WJ, Heron SF, Marsh BL, Liu G, De La Cour JL, Geiger EF, Eakin CM (2019) The relentless march of mass coral bleaching: a global perspective of changing heat stress. Coral Reefs 38:547–557

Smale DA, Wernberg T, Oliver ECJ, Thomsen M and others (2019) Marine heatwaves threaten global biodiversity and the provision of ecosystem services. Nat Clim Change 9: 306–312

Staehr PA, Borum J (2011) Seasonal acclimation in metabolism reduces light requirements of eelgrass (*Zostera marina*). J Exp Mar Biol Ecol 407:139–146

Strydom S, Murray K, Wilson S, Huntley B and others (2020) Too hot to handle: unprecedented seagrass death driven by marine heatwave in a World Heritage Area. Glob Change Biol 26:3525–3538

Thomsen MS, Mondardini L, Alestra T, Gerrity S and others (2019) Local extinction of bull kelp (*Durvillaea* spp.) due to a marine heatwave. Front Mar Sci 6:84

Thomson JA, Burkholder DA, Heithaus MR, Fourqurean JW, Fraser MW, Statton J, Kendrick GA (2015) Extreme temperatures, foundation species, and abrupt ecosystem change: an example from an iconic seagrass ecosystem. Glob Change Biol 21:1463–1474

Wahid A, Gelani S, Ashraf M, Foolad MR (2007) Heat tolerance in plants: an overview. Environ Exp Bot 61:199–223

Wernberg T, Bennett S, Babcock RC, De Bettignies T and others (2016) Climate-driven regime shift of a temperate marine ecosystem. Science 353:169–172

York PH, Gruber RK, Hill R, Ralph PJ, Booth DJ, Macreadie PI (2013) Physiological and morphological responses of the temperate seagrass *Zostera muelleri* to multiple stressors: investigating the interactive effects of light and temperature. PLOS ONE 8:e76377

Editorial responsibility: Just Cebrian, San Francisco, California, USA
Reviewed by: This and a previous version reviewed in MEPS by 2 anonymous referees

Submitted: December 3, 2023
Accepted: April 10, 2024
Proofs received from author(s): May 15, 2024